New construction design of a fluorescent imaging filter set based on TiO_2/SiO_2

H.H. Mai[1]

[1]VNU University of Science, Vietnam National University, 334 Nguyen Trai, Hanoi, Vietnam

Abstract. This study presents a new construction design of a filter set for fluorescent imaging applications. The filter set includes three filters: one excitation, one emission and one dichroic filter. The filters are DBR filters which consist of alternating thin film layers of TiO_2/SiO_2. A needle technique was applied as a synthesis method to optimize the spectral performances of the filters by adjusting a proper number of layers with controlling thickness. As a proof of concept, the filters are designed to maximize the signal-to-noise ratio of fluorescent emission from FITC 488 dye. The obtained results show that the optimized filters represent advanced spectral performance which can be used to improve the sensitivity and the imaging contrast in fluorescence microscopy.

1. Introduction

Thin film technology has been attracted a lot of attention in microscopy imaging [1–3]. Many devices such as short-pass filters, long-pass filters, passband filters, stopband filters, polarizers, beam splitters and reflectors are developed with the help of multilayer dielectric thin film technology. These devices consist of alternating layers of high and low refractive index materials with particular thicknesses. The thickness of the layers of material must be on the order of the wavelengths of visible light. They function based on the principle of multiple reflections and interferences between high and low index material interfaces [1,4–9]. Technically speaking, the performance of thin film filters can be altered by changing the characteristic of the component films i.e refractive index of layers and optical thicknesses [8,10–12]. DBR filter is a type of band-pass filters. In order to satisfy the interfering condition, their layers are defined as quarter-wave thick of the center wavelength. A DBR filter normally exhibits a very high reflectivity in a certain range of wavelengths around a center wavelength. This high reflection region is known as the DBR stopband, and is governed by the refractive index contrast between the constituent layers [1,10,12].

In fluorescent microscopy imaging, a fluorophore/fluorochrome, a type of fluorescent dye used to mark proteins, tissues, and cells with a fluorescent label, is commonly used. A fluorophore works by absorbing energy of high frequency illumination (wavelengths in the ultraviolet, violet, or blue region of the spectrum), commonly referred to as the excitation range. Afterwards, it re-emits energy at slightly lower frequencies (wavelengths in the green, red, or NIR region of the spectrum), commonly referred to as the emission range. Technically speaking, by selecting individual optical filters with the maximum amount of transmission at each of those wavelengths will ensure brilliant fluorescent images. To maximize the possible brightness while maintaining high contrast in fluorescent optical imaging, a filter set which contains an excitation filter, an emission filter, and a dichroic filter or beamsplitter is normally used in fluorescent microscopy (Figure 1). The excitation filter is to filter out all wavelengths of the light source, except for the excitation range of the fluorophore under inspection.

The emission filter is to filter out the entire excitation range of the fluorophore under inspection, and to transmit the emission range of that fluorophore. The minimum transmission in the outer ranges of the excitation range and of the emission range of the excitation filter, and of the emission filter, respectively will dictate the brightness and brilliance of images. The dichroic filter or beamsplitter is placed in between the excitation filter and emission filter, at a 45° angle. Its purpose is to reflect the excitation signal towards the fluorophore under inspection, and to transmit the emission signal towards the detector. An ideal dichroic filter will have a sharp transition between maximum reflection and maximum transmission with a reflection of above 95% for the bandwidth of the excitation filter, and a transmission of above 90% for the bandwidth of the emission filter. In fluorescent imaging microscopy, a filter set which can maximize signal collection efficiency is always of high demand.

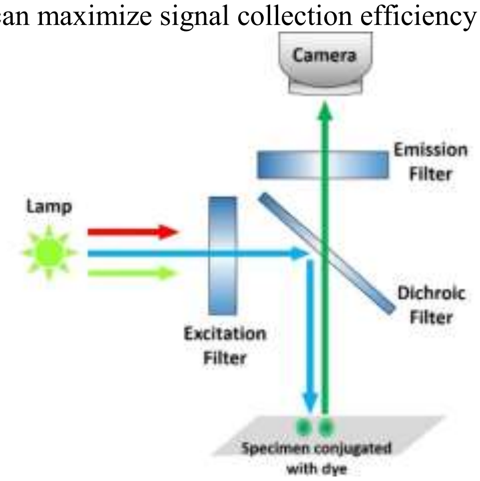

Figure 1. A typical filter set in a fluorescent microscope setup including an excitation filter, an emission filter and a dichroic filter.

In this work, the designs of DBR filters based on TiO_2/SiO_2 are proposed for a filter set for fluorescence microscopy imaging. As a proof of concept, the filter set was typically designed for fluorescein isothiocyanate 488 (FITC 488) dye which is normally used as a marker substance for the visualization and for the detection of tissue-bound bio molecules like e.g. antigens, lectins, various proteins, peptides, nucleic acids, oligo- and polysaccharides in samples of human origin. Based on refractive indices and absorption coefficient of the materials, TiO_2 is selected for its high refractive index, while SiO_2 are selected material for its low refractive indices at the excitation and emission range of the dye. Open-source software, Open Filters, is used in this work to design and optimize the required filter, it uses transfer matrix method to analyze transmission and reflection of light from layers based on thicknesses and type of materials. For the excitation filter and the emission filter, the designs are optimized to maximum transmission in the excitation range and emission range while minimize transmission in the outer range by nm using needle synthesis method. Similarly, the needle method was also applied to optimize the dichroic filter which maximizes reflection for the bandwidth of the excitation filter and maximize transmission for the bandwidth of the emission filter.

2. Optimization of multilayer filters

The needle method was first described by Tikhonravov in 1982 [13]. The essence of needle technique is that using an algorithm to identify convenient places to insert new layers that will improve the discrepancy between the target and solution which is well known as merit function. Technically speaking, the optimal position of needle to be added is where derivative of merit function is negative. Mostly a few single needle layers are added and transmission/reflection spectrum is calculated. The addition of needle layers stops at the point where there is no improvement in the target transmission/reflection spectrum.

Since the excitation filter, emission filter, and dichroic filter are based on the DBR filter design, thus an initial DBR design with $H(LH)^p$ layer configureuration close to the required design is used [3,7,14–16]. In this configureuration, H and L are quarter-wave thick of high and low refractive index layers and p is the number of repeated high and low refractive index pairs. The high refractive index is denoted for TiO_2, and low refractive index is denoted for SiO_2. In this work, the material absorbance is considered as neglected.

Since FITC 488 dye requires maximum excitation wavelength of 490 nm, thus, in this work, an excitation filter having maximum transmission excitation range of 450 nm to 500 nm was selected to design. The emission band of FITC 488 is in the range of 500 nm to 550 nm which also defines the emission band of the emission filter.

2.1. Excitation filter design

The excitation filter was designed by combining two DBR filters with two different center wavelength of 400 nm and 560 nm. The number of repeated high and low index pair *p* of the two DBR filters are 9. The angle of the incident light was chosen as 0^o degrees. Note that, the transmitted light selected as unpolarized light. The transmission spectrum of the initial excitation filter design is presented in Figure. 2 showing in a transmission band of approx. 30 nm with rather low transmittance (dash line). Outsides the excitation range, even though the transmittance is low in the range of 300 nm up to 600 nm, but still rather high in the range of above 600 nm. That means the filter not only transmit light in the excitation range but also in another range which might lead to noise signal. This will create a significant impact on the low sensitivity and low contrast of microscopy imaging. By using needle function, an optimized DBR filter design (solid line) with 35 layers and total thickness of 2365 nm was obtained. Compared to the initial design, the optimized excitation filter exhibits a lightly broader band of 50 nm with significantly higher transmittance of 0.9. Furthermore, the fringes outside the excitation range are significantly suppressed. The data of the optimized DBR filter design is presented in Table 1.

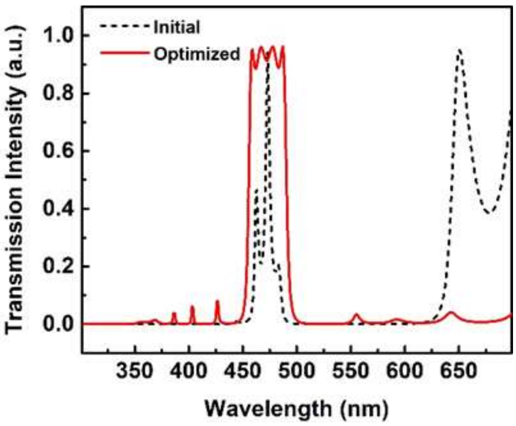

Figure 2. Transmission spectra of the initial and the optimized excitation filter. The incident angle is 0^o.

2.2. Emission filter design

Figure 3. represents the transmission spectrum of the initial (dash line) and optimized design (solid line) of the emission filter. Similarly, the emission filter was designed by combining two DBR filters with two different center wavelength of 450 nm and 640 nm to obtain an emission band from 500 nm to 550 nm. The number of repeated high and low index pair *p* of the two DBR filters are 9. The incident light was set as unpolarized and the incident angle was of 0^o. The initial designs show an emission band of 30 nm with high fluctuation in transmittance in the range of 510 nm to 550 nm. Another emission band is also observed in shorter range (from 350 nm to 400 nm). This denote that the filter cannot filter out all other wavelength outside of the desired wavelength band. By using needle function, an optimized FP filter design with 37 layers and total thickness of 2739 nm was obtained. Compared to the initial design, a broader emission band of 50 nm is observed with high transmittance approx. 0.9. Most importantly, the other band is suppressed. This allows the fluorescent emission of FITC 488 dye can be transmitted thoroughly the emission filter without attenuation. The data of the optimized emission filter design is presented in Table 2.

Table 1. Layer thickness of the optimized TiO_2/SiO_2 based excitation filter.

Layer No.	Material	Thickness (nm)	Layer No.	Materials	Thickness (nm)
1	TiO_2	59.68	19	TiO_2	109.79
2	SiO_2	3.26	20	SiO_2	91.69
3	TiO_2	36.35	21	TiO_2	59.23
4	SiO_2	80.69	22	SiO_2	95.56
5	TiO_2	47.85	23	TiO_2	55.15
6	SiO_2	81.08	24	SiO_2	95.41
7	TiO_2	35.94	25	TiO_2	68.61
8	SiO_2	33.79	26	SiO_2	101.73
9	TiO_2	43.06	27	TiO_2	52.79
10	SiO_2	75.96	28	SiO_2	92.76
11	TiO_2	32.45	29	TiO_2	74.26
12	SiO_2	45.94	30	SiO_2	63.77
13	TiO_2	46.01	31	TiO_2	37.51
14	SiO_2	85.36	32	SiO_2	79.60
15	TiO_2	55.13	33	TiO_2	86.72
16	SiO_2	96.26	34	SiO_2	104.94
17	TiO_2	94.94	35	TiO_2	52.90
18	SiO_2	89.21			

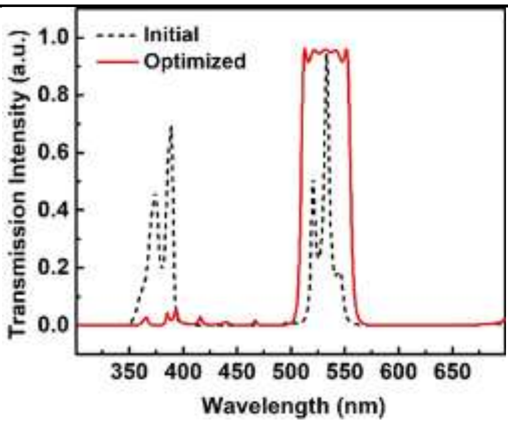

Figure 3. Transmission spectra of the initial and the optimized emission filter. The incident angle is 0°.

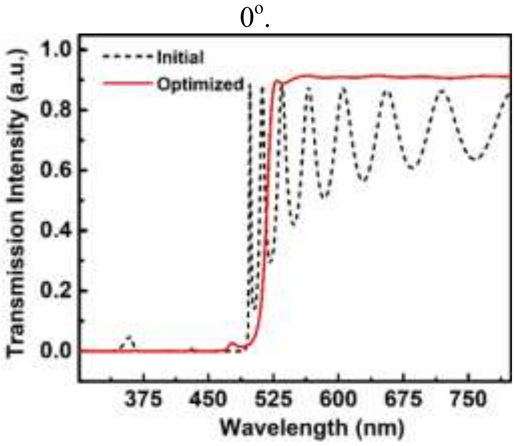

Figure 4. Transmission spectra of the initial and the optimized dichroic filter. The incident angle is 45°.

Table 2. Layer thickness of the optimized TiO_2/SiO_2 based emission filter.

Layer No.	Material	Thickness (nm)	Layer No.	Materials	Thickness (nm)
1	TiO_2	52.80	20	SiO_2	152.63
2	SiO_2	76.03	21	TiO_2	61.62
3	TiO_2	30.25	22	SiO_2	126.63
4	SiO_2	56.48	23	TiO_2	51.95
5	TiO_2	45.26	24	SiO_2	81.75
6	SiO_2	81.11	25	TiO_2	78.23
7	TiO_2	47.34	26	SiO_2	77.84
8	SiO_2	81.80	27	TiO_2	84.28
9	TiO_2	47.45	28	SiO_2	101.49
10	SiO_2	80.48	29	TiO_2	89.88
11	TiO_2	44.01	30	SiO_2	95.02
12	SiO_2	59.56	31	TiO_2	46.50
13	TiO_2	33.45	32	SiO_2	97.51
14	SiO_2	66.83	33	TiO_2	63.22
15	TiO_2	49.86	34	SiO_2	116.19
16	SiO_2	102.08	35	TiO_2	90.84
17	TiO_2	66.69	36	SiO_2	84.61
18	SiO_2	73.17	37	TiO_2	80.83
19	TiO_2	63.34			

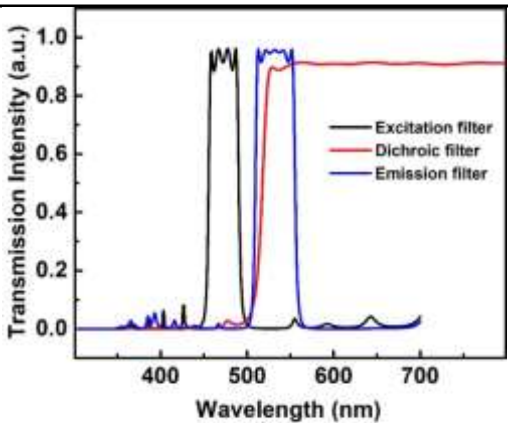

Figure 5. Transmission spectra of the filter set. The incident angle for the excitation and emission filter is 0° while and incident angle for the dichroic filter is of 45°.

2.3. Dichroic filter design

The excitation filter was designed as a DBR filter at center wavelength of 450 nm with *p* number is 20. Since the dichroic filter is used to reflect the excited light, and to transmit the emission light at the same time. Thus, the incident angle was set as 45°, the incident light was set as unpolarized. The transmission spectra of the initial (dash line) and optimized design (solid line) of the dichroic filter is presented in Figure 4. The initial filter exhibits nearly zero transmittance in the range below 500 nm which ensures to reflect all the excitation wavelengths. However, in the wavelength range above 500 nm, the filter presents high fluctuated transmittance which results in the partly transmitted emission wavelengths. In order to eliminate the fringes, the needle function was applied for designing optimized filter. Similar to the previous cases, the needle function significantly improves the spectra performance of the initial dichroic filter. As seen from the figure, the optimized filter maintains almost zero transmittance in the wavelength range of below 500 nm while exhibit high transmittance of approx.

0.9 in the range of above 500 nm. The total thickness of the optimized dichroic filter is of 2364 nm. The data of the optimized dichroic filter design is presented in Table 3. Figure 5. represents the transmittance of the filter sets in which the incident angle for the excitation and emission filter is 0^o while and incident angle for the dichroic filter is of 45^o.

Table 3. Layer thickness of the optimized TiO_2/SiO_2 based dichroic filter.

Layer No.	Material	Thickness (nm)	Layer No.	Materials	Thickness (nm)
1	TiO_2	25.61	17	TiO_2	50.14
2	SiO_2	65.51	18	SiO_2	82.59
3	TiO_2	52.89	19	TiO_2	35.03
4	SiO_2	54.47	20	SiO_2	86.68
5	TiO_2	26.08	21	TiO_2	71.85
6	SiO_2	41.21	22	SiO_2	10.94
7	TiO_2	27.34	23	TiO_2	84.40
8	SiO_2	70.08	24	SiO_2	271.14
9	TiO_2	46.50	25	TiO_2	173.95
10	SiO_2	76.94	26	SiO_2	45.11
11	TiO_2	41.61	27	TiO_2	170.97
12	SiO_2	82.20	28	SiO_2	136.03
13	TiO_2	46.23	29	TiO_2	17.83
14	SiO_2	80.91	30	SiO_2	69.10
15	TiO_2	41.79	31	TiO_2	62.98
16	SiO_2	80.56552	32	SiO_2	135

3. Conclusion

In this work filter set including an excitation filter, a dichroic filter, and an emission filter are designed for optimum fluorescent optical imaging of FITC 488 dye. The filters were based on TiO_2/SiO_2 DBR filter designs. It has been shown that by using the needle technique, the optimized filters exhibit outstanding properties in compare to that of the initial filter designs for example the filters exhibit high transmittance or reflectance in the desired range while significantly suppress the fringes in the outer range. The obtained results can be considered as an important base for the applications of optimized filter set in microscopy imaging.

4. Acknowledgement

This research was supported by the International Centre for Genetic Engineering and Biotechnology (ICGEB) through a grant to Dr. Hanh Hong Mai. Grant NO. CRP/VNM17-03.

5. References

[1] Editors, S. Thin-Film Optical Filters / S. Editors, E.R. Pike, K. College, M.J. Padgett, J. Molloy, D.M. Eds – Taylor & Francis Book, 2010.
[2] Marthinsen, H. Numerical Methods for Optical Interference Filters – Sci. Technol, 2009.
[3] Habib, M. Simulation of near Infrared interference bandpass filters for spectroscopic applications / M. Habib, A. Ullah // Int. Conf. Comput. Electron. Electr. Eng. ICE Cube - Proc., 2016. – P. 234-238. DOI: 10.1109/ICECUBE.2016.7495230.
[4] Butt, M.A. Multilayer dielectric stack notch filter for 450-700 nm wavelength spectrum / M.A. Butt, S.A. Fomchenkov // CEUR Workshop Proceedings. – 2017. – Vol. 1900. – P. 1-4. DOI: 10.18287/1613-0073-2017-1900-1-4.
[5] Butt, M.A. An approach to developing a Fabry-Perot filter by a single fabrication step for gas sensing applications / M.A. Butt, Y.S. Strelkov // Proc.SPIE, 2018.

[6] Butt, M.A. Biomedical bandpass filter for fluorescence microscopy imaging based on {TiO}2/{SiO}2and {TiO}2/{MgF}2dielectric multilayers / M.A. Butt, S.A. Fomchenkov, A. Ullah, P. Verma, S.N. Khonina // J. Phys. Conf. Ser. – 2016. – Vol. 741. – P. 12136. DOI: 10.1088/1742-6596/741/1/012136.
[7] Modelling of multilayer dielectric filters based on TiO2 / SiO2 and TiO2 /MgF2 for fluorescence microscopy imaging / M.A. Butt, S.A. Fomchenkov, A. Ullah, M. Habib, R.Z. Ali // Computer Optics. – 2016. – Vol. 40(5). – P. 674-678. DOI: 10.18287/2412-6179-2016-40-5-674-678.
[8] Butt, M.A. Dielectric-Metal-Dielectric (D-M-D) infrared ({IR}) heat reflectors / M.A. Butt, S.A. Fomchenkov, S.N. Khonina // J. Phys. Conf. Ser. – 2017. – Vol. 917. – P. 62007. DOI: 10.1088/1742-6596/917/6/062007.
[9] Elyutin, V.V. Cold mirror based on high-low-high refractive index dielectric materials / V.V. Elyutin, M.A. Butt, S.N. Khonina // CEUR Workshop Proc. – 2017. – Vol. 1900. – P. 5-9. DOI: 10.18287/1613-0073-2017-1900-5-9.
[10] Nazar, A. Design optical filters using two different synthesis approaches / A. Nazar, J. Kufa, 2011. – P. 3.
[11] de Denus-Baillargeon, M.-M. Developing high-performance reflective coatings for the tunable filter and the high-order interferometer of the 3D-NTT / M.-M. de Denus-Baillargeon, L. Abel-Tibérini, M. Lequime, C. Carignan, B. Épinat, J.-L. Gach, O. Hernandez, M. Marcelin // Soc. Photo-Optical Instrum. Eng. Conf. Ser. – 2008. – Vol. 7013. – P. 111. DOI: 10.1117/12.789498.
[12] Nazar, A. New Construction Stacks for Optimization Designs of Edge Filter / A. Nazar, A.H. Ali, N.A. Jasem // IOSR J. Appl. Phys. – 2016. – Vol. 8. – P. 20-26. DOI: 10.9790/4861-0803022026.
[13] Tikhonravov, A.V. Application of the needle optimization technique to the design of optical coatings / A.V Tikhonravov, M.K. Trubetskov, G.W. DeBell // Appl. Opt. – 1996. – Vol. 35. – P. 5493-5508. DOI: 10.1364/AO.35.005493.
[14] Tang, H. Preparation and Spectrum Characterization of a High Quality Linear Variable Filter / H. Tang, J. Gao, J. Zhang, X. Wang, X. Fu // Coatings. – 2018. – Vol. 8. – P. 308. DOI: 10.3390/coatings8090308.
[15] Jen, Y.-J. Design and Fabrication of a Narrow Bandpass Filter with Low Dependence on Angle of Incidence / Y.-J. Jen, M.-J. Lin // Coatings. – 2018. – Vol. 8. – P. 231. DOI: 10.3390/coatings8070231.
[16] de Denus-Baillargeon, M.-M. Design and fabrication of stress-compensated optical coatings: Fabry–Perot filters for astronomical applications / M.-M. de Denus-Baillargeon, T. Schmitt, S. Larouche, L. Martinu // Appl. Opt. – 2014. – Vol. 53. – P. 2616. DOI: 10.1364/AO.53.002616.